Contribution from the Department of Chemistry,
The University of Alberta, Edmonton, Alberta, Canada T6G 2G2

Preparation and Characterization of Some Binuclear DPM-Bridged Complexes of Iridium and the Structure of One Product, $[Ir_2Cl_2(CO)_2(\mu\text{-}CO)(Ph_2PCH_2PPh_2)_2]\cdot 3C_4H_8O$

BRUCE R. SUTHERLAND and MARTIN COWIE*

Received July 13, 1983

The reaction of bis(diphenylphosphino)methane (DPM) with $[IrCl(C_8H_{14})_2]_2$ under CO yields the binuclear complex $[Ir_2Cl(CO)_3(\mu\text{-}CO)(DPM)_2][Cl]$, and from this the BPh_4^- and BF_4^- salts can be readily prepared. Carbonyl loss from the chloro salt first yields two isomers of $[Ir_2Cl_2(CO)_2(\mu\text{-}CO)(DPM)_2]$ and finally *trans*-$[IrCl(CO)(DPM)]_2$, whereas CO loss from the BPh_4^- and BF_4^- salts gives $[Ir_2(CO)_2(\mu\text{-}Cl)(\mu\text{-}CO)(DPM)_2]^+$ with the corresponding anion. The dicarbonyl A-frame $[Ir_2(CO)_2(\mu\text{-}Cl)(DPM)_2]^+$ cannot readily be obtained via CO loss from the corresponding cationic tricarbonyl species but is easily obtained in the reaction of *trans*-$[IrCl(CO)(DPM)]_2$ with 1 equiv of $AgBF_4$. An X-ray structural determination of $[Ir_2Cl_2(CO)_2(\mu\text{-}CO)(DPM)_2]$ shows that the terminal carbonyl and chloro ligands are disordered. This disorder can be rationalized on the basis of the cocrystallization of two isomers, one in which all carbonyl groups are mutually cis (in approximately 25% abundance) and the other (75% abundance) in which the bridging carbonyl group is trans to a terminal carbonyl on one metal and to a chloro ligand on the other. These two isomers interconvert rapidly on the NMR time scale but can be discerned in infrared spectra. $[Ir_2Cl_2(CO)_2(\mu\text{-}CO)(DPM)_2]$ crystallizes with three molecules of THF in the space group $P2_1/c$ with $a = 22.890$ (6) Å, $b = 13.152$ (4) Å, $c = 22.129$ (5) Å, $\beta = 114.39$ (3)°, and $Z = 4$. The structure was refined to $R = 0.043$ and $R_w = 0.054$ on the basis of 5303 unique observed reflections and 268 parameters varied.

Introduction

There is considerable current interest in multinuclear metal complexes and in their reactions with small molecules, especially with regards to their potential catalytic activity and their relationship to reactions at metal surfaces.[1,2] The prototype multinuclear system is the binuclear one in which the two metals are in close proximity to one another. In such systems it is common to use bridging groups to hold the metals together in order to maintain the integrity of the complex during the course of reactions. One class of binuclear compounds that has been shown to display a rather diverse chemistry utilizes diphosphine ligands such as bis(diphenylphosphino)methane (DPM) or related phosphine groups to bind the two metals. Binuclear complexes bridged by such groups have been extensively studied for rhodium,[3-9] palladium,[10,11] and platinum[12,13] and more recently for mixed-metal systems involving one or more of these metals.[14,15] However, much less work has been done with iridium.[16,17]

We have recently extended our studies on binuclear, DPM-bridged complexes of rhodium[3-5,18-22] to that of iridium. One intention was to attempt the isolation and characterization of iridium complexes that bear a strong resemblance to potential intermediates in the analogous rhodium chemistry and, by so doing, obtain information about these labile rhodium intermediates. However, very early in our study it became apparent that significant differences existed in the natures and reactivities of the rhodium and iridium carbonyl precursors. Therefore, we undertook a detailed examination of the DPM-bridged iridium carbonyls in order to fully characterize the species involved and to offer a comparison with the well-established rhodium compounds. Herein, we report the results of this study.

Experimental Section

All solvents were appropriately dried and distilled prior to use and were stored under dinitrogen. Reactions were performed under standard Schlenk conditions (using dinitrogen that had previously been passed through columns containing Ridox and 4-Å molecular sieves to remove traces of oxygen and water, respectively). Hydrated iridium(III) chloride was obtained from Johnson-Matthey, and bis(diphenylphosphino)methane (DPM) was purchased from Strem Chemicals. Carbon monoxide was obtained from Matheson and used as received. $[IrCl(C_8H_{14})_2]_2$ was prepared by the reported procedure.[23] Variable-temperature $^{31}P\{^1H\}$ NMR spectra were run on Bruker HFX-90 spectrometer with Fourier transform capability operating at 36.43 MHz; the temperature was measured with a thermocouple inserted directly into the probe. NMR spectra were measured by using an external acetone-d_6 lock, and chemical shifts were referenced to 85% H_3PO_4. Infrared spectra were run on a Nicolet 7199 Fourier transform interferometer either as solids in Nujol mulls on KBr plates or as solutions in NaCl cells with 0.5-mm window path lengths. Analyses were performed by Canadian Microanalytical Service Ltd., Vancouver.

Preparation of Compounds. (a) $[Ir_2Cl(CO)_3(\mu\text{-}CO)(DPM)_2][Cl]$ (1a). Bis(diphenylphosphino)methane (171.1 mg, 0.445 mmol) was dissolved in 2 mL of CH_2Cl_2 under a slow stream of carbon monoxide. A solution of $[IrCl(C_8H_{14})_2]_2$ (200.0 mg, 0.222 mmol) in 10 mL of CH_2Cl_2 was then added dropwise from a syringe while the solution was rapidly stirred. The solution initially turned black but over a period of 5 min changed to red-orange and then to red, after which time the carbon monoxide flow was shut off and the solution allowed

---

(1) Krause, M. J.; Muetterties, E. L. *Angew. Chem., Int. Ed. Engl.* **1983**, *22*, 135.
(2) Band, E.; Bruker, C. F.; Muetterties, E. L.; Pretzer, W. R.; Rhodin, T. N. *Chem. Rev.* **1979**, *79*, 91.
(3) Cowie, M.; McKeer, I. R. *Inorg. Chim. Acta* **1982**, *65*, L107.
(4) Cowie, M.; Southern, T. G. *Inorg. Chem.* **1982**, *21*, 246.
(5) Cowie, M.; Dwight, S. K. *J. Organomet. Chem.* **1981**, *214*, 233.
(6) DeVries, S. H.; Mague, J. T. *Inorg. Chem.* **1980**, *19*, 3743 and references therein.
(7) DeVries, S. H.; Mague, J. T. *Inorg. Chem.* **1982**, *21*, 1632 and references therein.
(8) Eisenberg, R.; Kubiak, C. P.; Woodcock, C. *Inorg. Chem.* **1982**, *21*, 2119 and references therein.
(9) Eisenberg, R.; Kubiak, C. P. *Inorg. Chem.* **1980**, *19*, 2726.
(10) Balch, A. L.; Hunt, C. T.; Hunt, C. T.; Lee, C.-L. *Organometallics* **1982**, *1*, 824 and references therein.
(11) Balch, A. L.; Farr, J. P.; Hunt, C. T.; Lee, C.-L.; Olmstead, M. M. *J. Am. Chem. Soc.* **1981**, *103*, 3764 and references therein.
(12) Brown, M. P.; Fisher, J. R.; Frew, A. A.; Manojlović-Muir, L.; Mills, A. J.; Muir, K. W.; Puddephatt, R. J.; Sumner, S.; Thomson, M. A. *Organometallics* **1982**, *1*, 1421 and references therein.
(13) Azam, K. A.; Frew, A. A.; Lloyd, B. R.; Manojlović-Muir, L.; Muir, K. W.; Puddephatt, R. J. *J. Chem. Soc., Chem. Commun.* **1982**, 614 and references therein.
(14) McEwan, D. M.; Pringle, P. G.; Shaw, B. L. *J. Chem. Soc., Chem. Commun.* **1982**, 859.
(15) McDonald, W. S.; Pringle, P. G.; Shaw, B. L. *J. Chem. Soc., Chem. Commun.* **1982**, 861.
(16) Mague, J. T.; Sanger, A. R. *Inorg. Chem.* **1979**, *18*, 2060.
(17) Eisenberg, R.; Kubiak, C. P.; Woodcock, C. *Inorg. Chem.* **1980**, *19*, 2733.
(18) Cowie, M.; Dickson, R. S. *Inorg. Chem.* **1981**, *20*, 2682.
(19) Cowie, M.; Dwight, S. K. *Inorg. Chem.* **1980** *19*, 2508.
(20) Cowie, M.; Dwight, S. K. *Inorg. Chem.* **1980**, *19*, 209.
(21) Cowie, M.; Dwight, S. K. *Inorg. Chem.* **1979**, *18*, 2700.
(22) Cowie, M. *Inorg. Chem.* **1979**, *18*, 286.
(23) Herde, J. L.; Lambert, J. C.; Senott, C. V. *Inorg. Synth.* **1974**, *15*, 18.

0020-1669/84/1323-2324$01.50/0

Table I. Spectral Data

	IR^a ν(CO), cm^{-1}		
compd	solid^b	soln^c	$^{31}P\{^1H\}$ NMR δ^d
$[Ir_2Cl(CO)_3(\mu\text{-}CO)(DPM)_2][Cl]$ (**1a**)	2036 (m), 2001 (vs), 1979 (vs), 1764 (m)	2054 (s), 1999 (s), 1971 (vs), 1767 (m)	−6.32, −15.49 (m)^e
$[Ir_2Cl(CO)_3(\mu\text{-}CO)(DPM)_2][BF_4]$ (**1b**)	2034 (m), 2001 (s), 1981 (vs), 1761 (m)	2039 (m), 1999 (s), 1987 (vs), 1759 (m)	−6.32, −15.49 (m)^e
$[Ir_2Cl_2(CO)_2(\mu\text{-}CO)(DPM)_2]$ (**2**)	1980 (s), 1955 (vs, br), 1938 (sh), 1728 (s), 1704 (m)	1962 (vs, br), 1731 (m), 1717 (m)	−5.72 (s)
$[IrCl(CO)(DPM)]_2$ (**3**)	1953 (vs)	1954 (vs, br) (1999 (w)^f)	1.85 (8.69^f) (s)
$[Ir_2(CO)_2(\mu\text{-}Cl)(\mu\text{-}CO)(DPM)_2][BF_4]$ (4)	1971 (s), 1946 (vs), 1809 (s)	1973 (vs), 1941 (s), 1822 (m)	1.96 (s)
$[Ir_2(CO)_2(\mu\text{-}Cl)(DPM)_2][BF_4]$ (**5b**)	1989 (s), 1964 (vs)	1999 (s), 1976 (vs)	17.26 (s), 15.80^g (s), 12.07^h (s)

[a] IR abbreviations: vs = very strong; s = strong; m = medium; br = broad. [b] Nujol mulls. [c] In CH_2Cl_2 solution. [d] In CH_2Cl_2 solution unless otherwise noted. NMR abbreviations: s = singlet; m = multiplet. [e] See ref 6 for assignment of coupling constants. [f] Due to $[Ir_2(\mu\text{-}Cl)(CO)_2(DPM)_2][Cl]$. [g] In acetone. [h] In THF.

to stir under the CO atmosphere for an additional 15 min. During this time the color changed to pale yellow. The addition of 30 mL of diethyl ether, saturated with carbon monoxide, to the solution resulted in the precipitation of a pale yellow solid, which was collected and dried under a slow stream of CO. If THF was used as the solvent instead of CH_2Cl_2, the precipitate appeared after approximately 30 min without the addition of the ether. Compound **1** was determined to be a 1:1 electrolyte in CH_2Cl_2 solutions ($\Lambda(10^{-3}$ M) = 38.6 Ω^{-1} cm^2 equiv^{-1}). Typical isolated yields were 90–95%. Spectroscopic parameters for this and all subsequent products are given in Table I.

Anal. Calcd for $[Ir_2Cl(CO)_3(\mu\text{-}CO)(DPM)_2][Cl]$: C, 48.54; H, 3.32; Cl, 5.31. Found: C, 48.83; H, 3.18; Cl, 5.37.

(b) $[Ir_2Cl_2(CO)_2(\mu\text{-}CO)(DPM)_2]$ (2). A CH_2Cl_2 solution of $[Ir_2Cl(CO)_3(\mu\text{-}CO)(DPM)_2][Cl]$ was refluxed under a slow stream of N_2 until the color changed from light yellow to dark orange (approximately 20 min). The addition of 30 mL of degassed diethyl ether to the solution, after it had been allowed to cool to room temperature, resulted in the precipitation of a bright yellow microcrystalline product. The solid was collected and dried initially under a slow N_2 stream and finally by storing the sample under a slight vacuum for several hours. Recrystallization from a mixture of warm THF and diethyl ether yielded golden yellow crystals that contained both the cis and trans isomers (vide infra); attempts to separate the two by fractional crystallization and chromatography proved unsuccessful. Conductivity measurements on a CH_2Cl_2 solution of the crystalline material indicated the mixture was nonconducting ($\Lambda(10^{-3}$ M) = 2.2 Ω^{-1} cm^2 equiv^{-1}). Typical total yields of both isomers were 90–95%.

Anal. Calcd for $Ir_2Cl_2(CO)_2(\mu\text{-}CO)(DPM)_2$: C, 48.66; H, 3.39; Cl, 5.42. Found: C, 49.22; H, 4.39; Cl, 5.62.

(c) *trans*-$[IrCl(CO)(DPM)]_2$ (3). Method A. $[Ir_2Cl_2(CO)_5(\mu\text{-}CO)(DPM)_2]$ (200 mg, 0.153 mmol) was dissolved in 20 mL of THF and refluxed while a slow stream of dinitrogen was bubbled through the solution. The solution was heated for 1.5 h during which time the color changed from orange to red to dark red-purple. A red-purple solid finally precipitated. A 10-mL portion of degassed diethyl ether was added to ensure complete precipitation, and the solution was cooled for 20 min in an ice bath. The pale yellow mother liquor was removed, and the solid was collected, washed with several portions of ice-cold THF, and then dried in vacuo for 2 h. A CH_2Cl_2 solution of the red-purple solid showed that it was a nonelectrolyte ($\Lambda(10^{-3}$ M) = 3.1 Ω^{-1} cm^2 equiv^{-1}). Typical yields were 80–85%.

Anal. Calcd for $[IrCl(CO)(DPM)]_2$: C, 48.79; H, 3.46; Cl, 5.54. Found: C, 48.51; H, 3.40; Cl, 5.53.

Method B. If toluene was used instead of THF and the refluxing continued for 6 h, a maroon microcrystalline solid precipitated. This solid was collected, washed with diethyl ether, and dried in vacuo. Typical yields were 90–95%. In its spectroscopic properties and subsequent reactions with small molecules this product proved to be identical with the red-purple solid isolated in Method A. Preliminary X-ray photographs indicated that this species crystallized in the space group $P2_1/n$; a = 11.05 Å, b = 13.85 Å, c = 18.50 Å, and β = 93.16°. This unit cell volume of 2827.0 Å^3 and the measured density of 1.658 g/cm^3 corresponded to approximately Z = 2 and therefore suggested that the molecule had crystallographic $\bar{1}$ symmetry.

Anal. Calcd for $[IrCl(CO)(DPM)]_2$: C, 48.79; H, 3.46; Cl, 5.54. Found: C, 49.45; H, 3.44; Cl, 5.57.

(d) $[Ir_2(CO)_2(\mu\text{-}Cl)(\mu\text{-}CO)(DPM)_2][BF_4]$ (4b). Method A. $[Ir_2Cl(CO)_3(\mu\text{-}CO)(DPM)_2][BF_4]$ was prepared and isolated according to literature procedure[6,16] using $NaBF_4$ instead of $NaBPh_4$. A 200-mg portion (0.144 mmol) was then dissolved in 20 mL of CH_2Cl_2 under an N_2 atmosphere. The solution was refluxed for 45 min under a slow N_2 stream during which time the color changed from pale yellow to orange-yellow to golden orange. After the solution was cooled to room temperature, 30 mL of degassed diethyl ether was added to the solution, resulting in the precipitation of a golden orange solid. This solid was identical in all spectral and physical properties with that previously reported for the compound. Typical yields were 90–95%.

Method B. A 200-mg sample (0.153 mmol) of $[Ir_2Cl_2(CO)_2(\mu\text{-}CO)(DPM)_2]$ was dissolved in 10 mL of THF. To this solution was added a solution of 29.8 mg (0.153 mmol) of $AgBF_4$ in 2 mL of THF. The color immediately changed to golden orange, and a precipitate slowly appeared. This solution was stirred for 1 h, 30 mL of degassed diethyl ether was added to complete the precipitation, and the solid was collected and dried under a stream of N_2. The golden orange product was then redissolved in CH_2Cl_2, filtered under N_2, reprecipitated by adding diethyl ether, and collected and dried in vacuo for several hours. The product was identical in all spectroscopic properties with that obtained for the product from method A.

(e) $[Ir_2(CO)_2(\mu\text{-}Cl)(DPM)_2][BF_4]$ (5b). $[IrCl(CO)(DPM)]_2$ (200 mg, 0.156 mmol) was suspended in 10 mL of THF. To this slurry was added a solution of $AgBF_4$ (28.6 mg, 0.156 mmol) in 2 mL of THF. The color immediately changed to dark red, and after the mixture was stirred for 30 min, a coral-orange precipitate appeared. Addition of 30 mL of diethyl ether caused complete precipitation. After the solvent was removed and the solid was dried under an N_2 stream, the product was redissolved in 10 mL of CH_2Cl_2, filtered under dinitrogen, and reprecipitated by the addition of diethyl ether to give a dark red solid. Compound **5** was determined to be a 1:1 electrolyte in CH_2Cl_2 solutions ($\Lambda(10^{-3}$ M) = 47.2 Ω^{-1} cm^2 equiv^{-1}). Typical yields were 90–95%.

Anal. Calcd for $[Ir_2(CO)_2(\mu\text{-}Cl)(DPM)_2][BF_4]$: C, 46.91; H, 3.53; Cl, 2.82. Found: C, 46.27; H, 3.42; Cl, 2.63.

X-ray Data Collection. Bright yellow crystals of $[Ir_2Cl_2(CO)_2(\mu\text{-}CO)(DPM)_2]$ were obtained by slow cooling of a saturated THF/ether solution of **2**. A suitable crystal was mounted in the air on a glass fiber, immediately coated in a layer of epoxy, and then cooled to −40 °C to minimize CO loss. Unit cell parameters (at −40 °C) were obtained from a least-squares refinement of the setting angles of 23 reflections, in the range 16.3 ≤ 2θ ≤ 30.6°, which were accurately centered on an Enraf-Nonius CAD4 diffractometer using Mo Kα radiation. The systematic absences ($h0l$, l = odd; $0k0$, k = odd) were consistent with the space group $P2_1/c$.

Intensity data were collected at −40 °C on a CAD4 diffractometer in the bisecting mode employing the ω–2θ scan technique up to 2θ = 57.0° with graphite-monochromated Mo Kα radiation. Backgrounds were scanned for 25% of the peak width on either end of the peak scan. The intensities of three standard reflections were measured every 1 h of exposure to assess possible crystal decomposition or movement. No significant variation in these standards was noted, so no correction was applied to the data. A total of 8968 unique reflections were measured and processed in the usual way using a value of 0.04 for p;[24] of these, 5303 were considered to be observed and were

Table II. Summary of Crystal Data and Details of Intensity Collection

compd	$[Ir_2Cl_2(CO)_2(\mu\text{-}CO)(DPM)_2]\cdot 3C_4H_8O$
fw	1524.49
formula	$Ir_2Cl_2P_4O_6C_{65}H_{68}$
cell parameters	a = 22.890 (6) Å b = 13.152 (4) Å c = 22.129 (5) Å β = 114.39 (3)° V = 6075.61 Å^3
d(calcd), g/cm^3	1.666
space group	$P2_1/c$
temp, °C	−40
radiation (λ, Å)	graphite-monochromated Mo Kα (0.710 69)
receiving aperture, mm	2.00 + (0.500 tan θ) wide × 4.0 high, 173 from crystal
take-off angle, deg	1.7
scan speed, deg/min	variable between 10.058 and 1.804
scan width, deg	0.75 + (0.350 tan θ) in ω
2θ limits, deg	3.0 ≤ 2θ ≤ 57.0
no. of unique collcd	8968
no. of unique data used ($F_o^2 \geq 3\sigma(F_o^2)$)	5303
range of transmissn factors[25]	0.792–0.999
final no. of parameters refined	268
error in observn of unit weight	1.007
R	0.043
R_w	0.054

used in subsequent calculations. Since the crystal faces were obscured by the epoxy coating, an empiral absorption correction based on φ scans was used.[25] See Table II for pertinent crystal data and the details of data collection.

Structure Solution and Refinement. The structure was solved in the space group $P2_1/c$ by using standard Patterson and Fourier techniques. Atomic scattering factors for non-hydrogen[26] and hydrogen[27] atoms were taken from the usual sources. Anomalous dispersion terms for Ir, Cl, and P were included in F_c.[28] The carbon atoms of the DPM phenyl groups were refined as rigid groups having idealized D_{6h} symmetry, C–C distances of 1.392 Å, and independent isotropic thermal parameters. All hydrogen atoms were input as fixed contributions; their idealized positions were calculated after each cycle of refinement from the geometries of their attached carbon atoms by using a C–H distance of 0.95 Å. These hydrogen atoms were assigned isotropic thermal parameters of 1 Å^2 greater than the B (or equivalent isotropic B) of their attached carbon atom.

Although location of most atoms was straightforward, the chlorines and terminal carbonyl groups were found to be disordered such that only essentially spherical electron densities were located at distances from the Ir atoms corresponding to the approximate positions of the chlorine atoms and the midpoints of the CO groups. In attempts to resolve this disorder, the chlorine atoms were placed at the positions of the peak maxima and assigned occupancy factors based on the relative intensities of these peaks such that the total occupancy equaled 2. A difference Fourier map phased on all other atoms and these chlorine positions showed electron density in the approximate positions for carbonyl groups. However, subsequent attempts to refine the carbon and oxygen positions failed; these atoms invariably moved together, toward the chlorine positions, resulting in unreasonably short C–O distances. For this reason, the carbon and oxygen positions were idealized on either side of the Fourier peak corresponding to the chlorine position such that the Ir–C–O group was linear, with Ir–C and C–O distances of 1.82 and 1.15 Å, respectively. Many refinements were carried out in which the occupancy factors were correlated in a variety of ways, and all resulted in essentially the same result, i.e. that Cl(1) and C(1)–O(1) had occupancies near 50% (corresponding to 50% for Cl(1)′ and C(1)′–O(1)′) while Cl(2) and C(2)–O(2) had occupancies near 75% (corresponding to 25% for Cl(2)′ and C(2)–O(2)′). These occupancies proved to be consistent with the infrared spectrum, which could readily be explained on the basis of this information (vide infra), and so were fixed to these values in the remaining cycles. The thermal parameters of Cl(2)′, C(2)′, and O(2)′ did not behave well, so these were fixed at the average values observed for the other atoms of the same type. In the final refinements, the chlorine atom positions and isotropic thermal parameters were refined (apart from Cl(2)′ whose positional parameters were refined only) and the carbonyl thermal parameters were refined (apart from C(2)′ and O(2)′, which were not refined). In spite of the difficulty in resolving this disorder, all other parts of the molecule are well-defined. The chlorine atoms refined to acceptable values, and the positions of these and the CO groups with respect to other groups in the molecule are chemically resonable (vide infra). Furthermore, it is encouraging that the occupancy factors offer an explanation of the infrared data (vide infra).

In the final refinements the nondisordered atoms of the complex were refined anisotropically except for hydrogens, which were included as fixed contributions; the C and O atoms of the THF molecules were refined anisotropically. The hydrogen atoms of these solvent molecules were not included owing to the relatively high thermal parameters of the C and O atoms.

The final model with 268 parameters refined converged to R = 0.043 and R_w = 0.054.[29] On the final difference Fourer map the highest 20 peaks (2.51–1.56 e Å^{-3}) were in the vicinities of the disordered atoms, the phenyl groups, and the Ir and P atoms. A typical carbon atom on earlier syntheses had a peak intensity of about 9.5 e Å^{-3}.

The final positional parameters of the individual non-hydrogen atoms and the phenyl groups are given in Tables III and IV, respectively. The derived hydrogen positions, their thermal parameters, and a listing of observed and calculated structure amplitudes used in the refinements are available.[30]

Discussion

The reaction of $[IrCl(cyclooctene)_2]_2$ with DPM and CO results in a series of color changes from the initial orange solution to black, red, and finally a pale yellow solution. The black species initially formed is probably $[IrCl(CO)_3]_n$,[31] which then rapidly reacts with DPM to give the DPM-containing complexes, the final species of which is the pale yellow product **1**. $^{31}P\{^1H\}$ NMR and infrared spectra of this final species are essentially identical with those reported for $[Ir_2Cl(CO)_4(DPM)_2][BPh_4]$[6,16] (apart from the absence of any infrared stretches due to BPh_4^-). This, together with its conductivity, which indicates that it is a 1:1 electrolyte, and the elemental analysis, which shows the presence of 2 Cl atoms per dimer, suggests the formulation $[Ir_2Cl(CO)_4(DPM)_2][Cl]$ (**1a**).

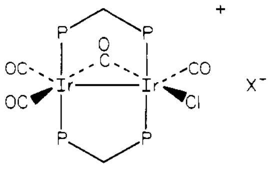

1a, X = Cl
b, X = BF$_4$
c, X = BPh$_4$

Although two structures have been suggested,[6,16] for this cation, the one shown, as proposed by Mague and DeVries[6] for the diarsine analogue based on a careful ^{13}CO-labeling study, is

---

(24) Doedens, R. J.; Ibers, J. A. *Inorg. Chem.* **1967**, *6*, 204.

(25) Besides local programs, the following were used in solution and refinement of the structure: BUCILS, structure factor and refinement program; FASTFO, a modified version of FORDAP, Fourier summation program by R. J. Dellaca; ORFFE for calculating bond lengths, angles, and associated deviations by W. Busing and H. A. Levy; ORTEP, plotting program by C. K. Johnson; EAC, empirical absorption program by A. C. T. North, D. C. Phillips, and F. S. Mathews from the Enraf-Nonius Structure Determination Package by B. A. Frenz.

(26) Cromer, D. T.; Weber, J. T. "International Tables for Crystallography"; Kynoch Press: Birmingham, England, 1974; Vol. IV, Table 2.2 A.

(27) Stewart, R. F.; Davidson, E. R.; Simpson, W. T. *J. Chem. Phys.* **1965**, *42*, 3175.

(28) Cromer, D. T.; Liberman, D. J. *J. Chem. Phys.* **1970**, *53*, 1891.

(29) $R = \sum||F_o| - |F_c||/\sum|F_o|$; $R_w = [\sum w(|F_o| - |F_c|)^2/\sum wF_o^2]^{1/2}$.

(30) Supplementary material.

(31) Peterson, S. W.; Reis, A. H. *Ann. N.Y. Acad. Sci.* **1978**, *313*, 560 and references therein.

Table III. Positional and Thermal Parameters for the Nongroup Atoms of $[Ir_2Cl_2(CO)_3(DPM)_2]\cdot 3C_4H_8O$

atom	x^a	y	z	B, Å^2	atom	x	y	z	B, Å^2
Ir(1)	0.25048 (3)	0.13450 (4)	0.04861 (3)	1.25^b	C(1)′	0.1990	0.1192	0.0926	3.9 (8)
Ir(2)	0.22651 (3)	0.33550 (4)	0.00698 (3)	1.19^b	C(2)	0.2366	0.4415	−0.0406	2.4 (4)
Cl(1)	0.1784 (4)	0.1255 (6)	0.1074 (4)	2.5 (2)	C(2)′	0.1814	0.3717	0.0549	2.5
Cl(1)′	0.3160 (4)	−0.0239 (8)	0.0506 (3)	2.1 (2)	C(3)	0.2782 (6)	0.2224 (10)	−0.0108 (7)	1.79^b
Cl(2)	0.1637 (2)	0.3760 (4)	0.0745 (3)	2.8 (2)	C(4)	0.3258 (7)	0.3140 (10)	0.1707 (6)	1.84^b
Cl(2)′	0.2428	0.4750	−0.0650	1.8 (4)	C(5)	0.0969 (6)	0.1783 (10)	−0.0630 (6)	1.89^b
P(1)	0.3320 (2)	0.1816 (2)	0.1506 (2)	1.44^b	C(T1)	0.247 (1)	−0.254 (2)	−0.146 (1)	5.9 (5)
P(2)	0.3129 (2)	0.3951 (2)	0.0997 (2)	1.39^b	C(T2)	0.3034 (8)	−0.2310 (11)	−0.1510 (8)	3.1 (3)
P(3)	0.1587 (2)	0.0783 (2)	−0.0403 (2)	1.43^b	C(T3)	0.356 (1)	−0.218 (2)	−0.094 (1)	5.7 (5)
P(4)	0.1276 (2)	0.2969 (3)	−0.0786 (2)	1.31^b	C(T4)	0.3388 (8)	−0.2659 (12)	−0.0390 (9)	3.8 (4)
O(1)	0.3259	−0.0487	0.0476	5.7 (1)	C(T5)	0.3960 (9)	0.0860 (16)	−0.1372 (11)	5.4 (5)
O(1)′	0.1666	0.1095	0.1204	4.6 (8)	C(T6)	0.441 (1)	0.112 (2)	−0.067 (2)	9.3 (8)
O(2)	0.2430	0.5085	−0.0707	3.8 (3)	C(T7)	0.502 (2)	0.145 (3)	−0.071 (2)	12.3 (8)
O(2)′	0.1528	0.3946	0.0851	4.5	C(T8)	0.496 (1)	0.124 (2)	−0.143 (1)	6.4 (5)
O(3)	0.3096 (4)	0.2136 (6)	−0.0424 (5)	1.83^b	C(T9)	0.074 (1)	−0.093 (2)	0.246 (1)	8.4 (7)
O(T1)^c	0.2646 (9)	−0.2446 (14)	−0.0676 (9)	9.7 (5)	C(T10)	0.138 (1)	−0.047 (2)	0.248 (1)	7.9 (6)
O(T2)	0.4288 (7)	0.1155 (11)	−0.1781 (8)	6.5 (4)	C(T11)	0.159 (1)	−0.112 (2)	0.205 (1)	6.8 (6)
O(T3)	0.0480 (7)	−0.1286 (11)	0.1771 (8)	6.4 (3)	C(T12)	0.099 (2)	−0.148 (3)	0.156 (2)	14.3 (13)
C(1)	0.2967	0.0222	0.0480	1.8 (6)					

^{a} Estimated standard deviations in the last significant figure(s) are given in parentheses in this and all subsequent tables. ^{b} Equivalent isotropic B's for anisotropic atoms. U_{ij}'s and associated standard deviations are listed in the supplementary material. ^{c} The THF solvent molecules are labeled as follows: THF(1), O(T1), C(T1), C(T2), C(T3), C(T4); THF(2), O(T2), C(T5), C(T6), C(T7), C(T8); THF(3), O(T3), C(T9), C(T10), C(T11), C(T12).

Table IV. Derived Parameters for the Rigid Groups of $[Ir_2Cl_2(CO)_3(DPM)_2]\cdot 3C_4H_8O$

atom	x	y	z	B, Å^2	atom	x	y	z	B, Å^2
C(11)	0.3282 (4)	0.1135 (6)	0.2212 (4)	1.4 (2)	C(51)	0.1617 (4)	0.0409 (7)	−0.1182 (4)	1.5 (2)
C(12)	0.3279 (5)	0.1651 (5)	0.2760 (5)	2.3 (3)	C(52)	0.2197 (3)	0.03302 (7)	−0.1242 (4)	1.9 (3)
C(13)	0.3260 (5)	0.1109 (7)	0.3292 (4)	2.7 (3)	C(53)	0.2205 (4)	0.0046 (8)	−0.1845 (5)	2.5 (3)
C(14)	0.3244 (5)	0.0051 (7)	0.3276 (4)	2.8 (4)	C(54)	0.1632 (5)	−0.0159 (8)	−0.2388 (4)	2.9 (3)
C(15)	0.3246 (5)	−0.0464 (5)	0.2728 (5)	2.6 (3)	C(55)	0.1052 (4)	−0.0080 (8)	−0.2328 (4)	2.8 (4)
C(16)	0.3266 (5)	0.0078 (6)	0.2196 (4)	2.2 (3)	C(56)	0.1044 (3)	0.0204 (8)	−0.1726 (5)	2.2 (3)
C(21)	0.4325 (4)	0.1621 (8)	0.1112 (3)	1.9 (3)	C(61)	0.1189 (4)	−0.0323 (6)	−0.0242 (5)	1.8 (2)
C(22)	0.4156 (3)	0.1664 (7)	0.1648 (4)	1.5 (2)	C(62)	0.0527 (4)	−0.0360 (7)	−0.0452 (5)	2.8 (3)
C(23)	0.4632 (5)	0.1686 (8)	0.2292 (4)	2.5 (3)	C(63)	0.0233 (3)	−0.1259 (8)	−0.0394 (6)	3.4 (4)
C(24)	0.5275 (4)	0.1665 (9)	0.2400 (4)	3.0 (4)	C(64)	0.0602 (5)	−0.2121 (7)	−0.0126 (6)	3.6 (4)
C(25)	0.5444 (3)	0.1621 (9)	0.1864 (5)	3.3 (4)	C(65)	0.1264 (5)	−0.2084 (6)	0.0084 (6)	3.6 (4)
C(26)	0.4968 (5)	0.1599 (9)	0.1220 (4)	2.9 (4)	C(66)	0.1558 (3)	−0.1185 (8)	0.0026 (5)	2.6 (3)
C(31)	0.3014 (5)	0.5228 (5)	0.1261 (5)	1.4 (2)	C(71)	0.0668 (4)	0.3896 (6)	−0.0846 (5)	1.4 (2)
C(32)	0.3112 (5)	0.6045 (7)	0.0914 (4)	3.0 (4)	C(72)	0.0113 (5)	0.3646 (6)	−0.0765 (5)	2.3 (3)
C(33)	0.3014 (5)	0.7034 (6)	0.1077 (5)	2.8 (4)	C(73)	−0.0336 (4)	0.4395 (8)	−0.0822 (6)	3.8 (4)
C(34)	0.2819 (5)	0.7206 (5)	0.1586 (5)	2.5 (3)	C(74)	−0.0231 (5)	0.5394 (7)	−0.0961 (6)	3.6 (4)
C(35)	0.2721 (5)	0.6389 (8)	0.1933 (5)	3.2 (4)	C(75)	0.0323 (5)	0.5643 (5)	−0.1042 (6)	2.8 (4)
C(36)	0.2819 (5)	0.5399 (6)	0.1771 (5)	2.4 (3)	C(76)	0.0772 (4)	0.4894 (7)	−0.0985 (5)	2.3 (3)
C(41)	0.3909 (3)	0.4090 (7)	0.0970 (5)	1.7 (2)	C(81)	0.1186 (4)	0.2889 (7)	−0.1642 (3)	1.8 (2)
C(42)	0.4450 (5)	0.4298 (8)	0.1548 (4)	2.2 (3)	C(82)	0.0570 (3)	0.2903 (7)	−0.2147 (5)	1.8 (3)
C(43)	0.5044 (4)	0.4423 (9)	0.1523 (4)	3.3 (4)	C(83)	0.0483 (3)	0.2811 (8)	−0.2806 (4)	2.2 (3)
C(44)	0.5097 (4)	0.4340 (9)	0.0920 (6)	3.3 (4)	C(84)	0.1011 (5)	0.2705 (8)	−0.2960 (3)	2.9 (4)
C(45)	0.4555 (5)	0.4133 (9)	0.0342 (4)	3.2 (4)	C(85)	0.1627 (4)	0.2691 (8)	−0.2455 (5)	2.7 (4)
C(46)	0.3962 (4)	0.4008 (8)	0.0368 (4)	1.6 (3)	C(86)	0.1715 (3)	0.2783 (7)	−0.1796 (4)	1.8 (3)

	$X_c{}^a$	Y_c	Z_c	φ	θ	ρ
ring 1	0.3263 (3)	0.0593 (5)	0.2744 (3)	3.127 (8)	2.603 (5)	1.549 (7)
ring 2	0.4800 (3)	0.1643 (5)	0.1756 (3)	−1.621 (9)	2.351 (5)	1.628 (9)
ring 3	0.2917 (3)	0.6217 (5)	0.1424 (3)	2.517 (14)	−2.019 (6)	0.844 (14)
ring 4	0.4503 (3)	0.4215 (5)	0.0945 (3)	1.929 (15)	2.039 (5)	−1.773 (15)
ring 5	0.1624 (3)	0.0125 (5)	−0.1785 (3)	1.639 (6)	−3.135 (5)	−1.843 (6)
ring 6	0.0896 (3)	−0.1222 (5)	−0.0184 (3)	−2.038 (6)	−3.106 (7)	0.296 (7)
ring 7	0.0218 (3)	0.4645 (5)	−0.0904 (3)	−0.697 (6)	2.664 (7)	2.899 (7)
ring 8	0.1099 (3)	0.2797 (4)	−0.2301 (3)	−1.637 (6)	3.015 (5)	−1.475 (6)

^{a} X_c, Y_c, and Z_c are the fractional coordinates of the centroid of the rigid group.

most probably correct. In further support of our formulation for the chloro salt (**1a**), the analogous compounds (**1b**,**c**) containing the noncoordinating anions BF_4^- and BPh_4^- can be readily prepared from **1a** by inducing precipitation in the presence of these larger anions, although the BF_4^- salt is best prepared by reacting **1a** with $AgBF_4$. Furthermore, carbonyl loss from **1a** yields the dichloro tricarbonyl species $[Ir_2Cl_2(CO)_3(DPM)_2]$, which has been completely characterized and has been shown by an X-ray structure analysis to display a geometry very similar to that proposed for **1** (vide infra). Compound **1a** presents an interesting contrast to the somewhat analogous DPM-bridged rhodium carbonyl compounds where the highest carbonyl-containing species is the tricarbonyl cation,[22,32] $[Rh_2(CO)_2(\mu\text{-}Cl)(\mu\text{-}CO)(DPM)_2]^+$. In the present case the more basic Ir centers allow the coordination of one more π-acid carbonyl group than the analogous Rh compounds.

Previous studies have usually utilized the above tetracarbonyl species, with noncoordination anions, as a precursor

---

(32) Cowie, M.; Mague, J. T.; Sanger, A. R. *J. Am. Chem. Soc.* **1978**, *100*, 3628.

for the preparation of DPM-bridged binuclear iridium complexes.[6,17] However, we have found that **1a**, with the chloride counterion, proves to be a more versatile starting material in the preparation of both neutral and charged binuclear carbonyl products (vide infra). Like its BPh_4^- analogue, **1a** readily loses CO even in the solid state and must be stored under an atmosphere of CO. However, CO loss from the solid is usually inefficient, leaving some of the tetracarbonyl starting material. Carbonyl loss is more conveniently carried out in refluxing CH_2Cl_2 in which the color changes to dark orange after about 20 min. The $^{31}P\{^1H\}$ NMR spectrum of this sample shows only one peak, a singlet at −5.72 ppm. An infrared spectrum of this solution shows a very broad band at 1962 cm^{-1} and two bands at 1731 and 1717 cm^{-1}. The solid precipitate obtained from this solution displays three bands in the terminal carbonyl region, at 1980 (s), 1955 (br, vs), and 1938 (sh) cm^{-1} and two bridging carbonyl bands at 1728 and 1704 cm^{-1}. Some insight into the origin of these bands, when only one species is observed in the $^{31}P\{^1H\}$ NMR spectrum, is obtained from the X-ray structure of **2**, which shows that each metal has one chloro and one terminal ligand and that both metals share a bridging carbonyl group. The terminal Cl and CO groups are disordered such that the two species present in the solid (**2a**,**b**) are those shown below. The infrared spectra can then be readily explained as arising from a mixtue of these two isomers. In solution, the bands in the terminal CO region broaden and coalesce to a single broad peak although the bridging bands remain resolved. In the solid state, however, all bands are resolved. Both isomers would be expected to give rise to different infrared spectra; in **2a** all carbonyls are cis whereas in **2b** the bridging CO is almost trans to one terminal CO but cis to the other.

In the solid the infrared stretches for the bridging carbonyl groups can be readily assigned on the basis of their relative intensities and the relative abundance of the two isomers **2a** and **2b**, as determined from the X-ray study. The band at 1728 cm^{-1} is several times more intense than that at 1704 cm^{-1} and so can be attributed to **2b**, the more abundant isomer in the crystal (see Description of Structure). Unfortunately, we are unable to unambiguously assign the terminal carbonyl bands. Only three terminal carbonyl stretches are observed although four are expected due to the two terminal CO groups on each isomer; presumably the broad intense band at 1955 cm^{-1} conceals two stretches. Attempts to correlate these terminal carbonyl bands with the bridging ones by varying the isomer ratios on crystallizing at different temperatures (−80 to +40 °C) did not succeed; although slight variations in band intensities were observed, we were unable to correlate the changes in a satisfactory manner.

In THF solution the bridging carbonyl bands of redissolved samples of **2** are of comparable intensity, suggesting essentially equal concentrations of **2a** and **2b**. We suggest that in solution species **2a** and **2b** readily interconvert through the ionic intermediate **4a**, by chloride loss and subsequent recoordination.

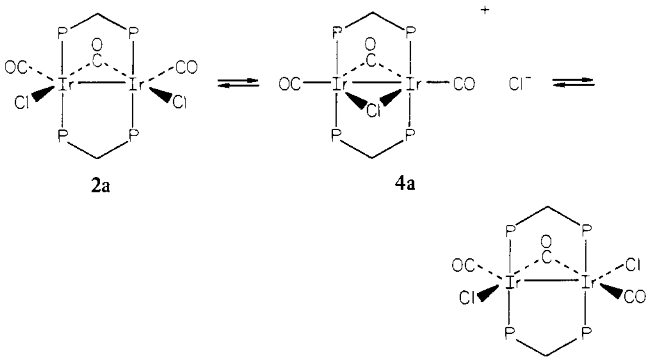

2a

4a

2b

Chloride recoordination in the proposed ionic intermediate can occur adjacent either to the bridging CO or to the bridging Cl; the former will yield **2b**, and the latter will yield **2a**. Compound **4** with noncoordinating anions has been prepared by ourselves and others[6,16] and has a bridging carbonyl band at ca. 1822 cm^{-1}. This band is *not* observed in the solution infrared spectrum of **2**, suggesting that the species is present in quantities too small to be detected. Consistent with this, solutions of **2** are nonconducting. The $^{31}P\{^1H\}$ NMR data suggests that **2a** and **2b** are interconverting rapidly on the NMR time scale; even at −80 °C there is no obvious change in the spectrum from that run at 20 °C. Support for the postulation of **4a** as the intermediate in this exchange comes from the addition of a solution of $Me_4N^+Cl^-$ to an acetone solution of the BF_4^- salt of **4**; a rapid reaction occurs to produce a mixture of **2a** and **2b** as identified by ^{31}P NMR and infrared spectroscopy. Additional support for the isomerism that we suggest is found in the work of Mague[6] where the reaction of **4** (as the BPh_4^- salt) with CN-*t*-Bu yields $[Ir_2Cl(CN\text{-}t\text{-}Bu)(CO)_2(\mu\text{-}CO)(DPM)_2]^+$ in which the infrared band due to the bridging CO group is reported to be somewhat asymmetric, suggesting two isomers of the type that we propose for **2a** and **2b**. The rapid interconversion of the two isomers (**2a** and **2b**) in solution also explains our inability to separate them either by chromatography or by fractional crystallization.

Compound **2** is very moisture and air sensitive in solution, and even the solid decomposes after several hours in air. This species also loses CO quite readily, and crystals left overnight under a recirculating N_2 atmosphere in a glovebox turned red on their surface due to CO loss (vide infra).

Refluxing compound **2** in THF results in the formation of a red-purple solid whereas refluxing in toluene yields a maroon solid. Although these two differ in appearance and in solubility (the red-purple solid is moderately soluble in CH_2Cl_2 and the maroon solid is very insoluble in solvents such as $CHCl_3$, CH_2Cl_2, acetone, THF, and toluene), they both appear to be the same species, *trans*-$[IrCl(CO)(DPM)]_2$ (**3**). The analogous rhodium dicarbonyl species also has been observed to crystallize in different crystal modifications in which the solubilities of the different forms differ.[33-36] Both forms of **3** react with small molecules (such as H_2,[37] acetylenes,[38] and heteroallenes[39]) to give identical products, offering further confirmation that they are the same compound. Although there is an earlier report of this compound,[40] it does not seem to have been obtained in a pure form. It was reported to have been obtained as a yellow solid from the reaction of $[IrCl(COD)]_2$ and DPM in 1:2 stoichiometries under an atmosphere of CO. When it was dried in vacuo, it was reported that this species lost benzene of crystallization to become a red-orange product. On the basis of our results, it seems more likely that the initial product was the tetracarbonyl complex or a mixture of it and the tricarbonyl species, which then lost CO in vacuo to give a mixture of these species and compound **3**. The mixture would explain the red-orange color instead of the bright red-purple or maroon colors we observe. In all of our studies the reactions were carefully monitored by $^{31}P\{^1H\}$ NMR and infrared spectroscopy, so it is clear in all cases how many major phosphorus-containing species are present.

Both samples of **3** show a single broad carbonyl band at 1953 cm^{-1} in the infrared spectra of the solids; however, dichloromethane solutions of the red-purple product shows a

---

(33) Cowie, M.; Dwight, S. K. *Inorg. Chem.* **1981**, *20*, 1534.
(34) Cowie, M.; Dwight, S. K. *Inorg. Chem.* **1980**, *19*, 2500.
(35) Mague, J. T. *Inorg. Chem.* **1969**, *8*, 1975.
(36) Balch, A. L., private communication.
(37) Cowie, M.; Sutherland, B. R., manuscript in preparation.
(38) Cowie, M.; Sutherland, B. R., submitted for publication.
(39) Cowie, M.; Loeb, S. J., unpublished results.
(40) Sanger, A. R. *J. Chem. Soc., Dalton Trans.* **1977**, 1971.

broad band at 1954 cm^{-1} and a smaller peak at 1999 cm^{-1}. This smaller band was observed in the original report[40] and was attributed to distortions of the compound from the ideal C_{2h} symmetry such that both carbonyl bands (B_u and A_g) became infrared active. We find instead that this smaller band is due to small amounts of an additional species **5a**. In the $^{31}P\{^1H\}$ NMR spectrum both species are clearly observed, the major one at δ 1.85 and the minor one (in approximately 10% abundance) at δ 8.69. We propose that this minor species is $[Ir_2(CO)_2(\mu\text{-}Cl)(DPM)_2][Cl]$ (**5a**), which is in equilibrium with **3** in solution. The analogous BF_4^- salt (**5b**) has infrared bands at 1999 and 1976 cm^{-1} in CH_2Cl_2 (see Table I) so that the lower frequency band of **5a** in CH_2Cl_2 solutions of **3** could easily be obscured by the broad band arising due to **3** at 1954 cm^{-1} (in fact, the band at 1954 cm^{-1} is unsymmetrical, suggesting the presence of a weak shoulder at ca. 1970 cm^{-1}). Although the $^{31}P\{^1H\}$ chemical shift of **5a** with the chloro counterion is different from that observed with BF_4^- (**5b**) (δ 8.69 and 17.26, respectively), such shift differences have been observed previously on changing from coordinating to noncoordinating anions.[41] Furthermore, the chemical shift of **5b** is found to be extremely solvent dependent (vide infra), so it is not surprising that the presence of a coordinating anion has a significant effect. In support of our formulation for **5a**, we have observed significant quantities of the analogous rhodium compound, $[Rh_2(CO)_2(\mu\text{-}Cl)(DPM)_2][Cl]$, in solutions of *trans*-$[RhCl(CO)(DPM)]_2$.[42] Although in solution species **3** and **5a** are in equilibrium, an infrared spectrum of the solid obtained from the solution shows only a single band at 1953 cm^{-1} due to **3**, indicating that Cl^- recoordination has occurred in **5a**. Furthermore, the reaction of mixtures of **3** and **5a** with small molecules such as acetylenes results in the formation of only one product.[38]

Compound **3** can have two possible geometries: a trans form (**3a**) or a cis form (**3b**). The spectral data do not rule out either possibility since without an Ir–Ir bond the carbonyl stretches need not be coupled, in which case there would be only one carbonyl stretch for both isomers. Preliminary X-ray photos of **3** indicate that it crystallizes in the space group $P2_1/n$ with $Z \simeq 2$ so the molecules are required to have $\bar{1}$ crystallographic symmetry.[43] This is the symmetry found for the molecules in all determinations of $[RhCl(CO)(L_2)]_2$ (L_2 = DPM, $Ph_2AsCH_2AsPh_2$).[33-35] Although compound **3** could have cis carbonyl groups and be disordered in the solid, we feel that the cis isomer is unlikely. In addition, the reaction of **4** with dimethylacetylenedicarboxylate yields an acetylene adduct whose geometry (determined by an X-ray structure) is consistent with a trans configuration in the starting material[38] (although supportive, this does not offer unambiguous proof since chloride loss, rearrangement, and chloride recoordination cannot be ruled out).

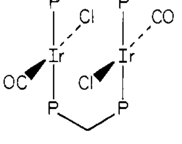

3a

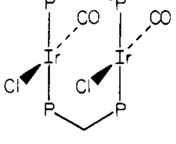

3b

Compound **3** is air sensitive in solution and turns from purple to yellow-green within 1–2 h upon exposure to air. A $^{31}P\{^1H\}$ NMR spectrum of this green-yellow solution shows that the major species appears as a singlet at δ −16.1, and its IR spectrum displays a new carbonyl stretch at 2020 cm^{-1}. Work is presently under way to characterize this species.

We have shown that successive carbonyl loss can be effected from $[Ir_2Cl(CO)_4(DPM)_2][Cl]$, yielding first $[Ir_2Cl_2(CO)_2(\mu\text{-}CO)(DPM)_2]$ and then $[IrCl(CO)(DPM)]_2$. On the basis of the analogous Rh–DPM system[19] it might be expected that further CO loss should occur to produce $[Ir_2Cl_2(\mu\text{-}CO)(DPM)_2]$. However, all attempts to prepare this complex have failed; the basic iridium centers are more reluctant to lose carbonyl groups than are the rhodium centers in the analogous rhodium complexes. Carbonyl loss from the above tetracarbonyl and tricarbonyl species is reversible, so under CO compound **3** yields **2** and ultimately **1a**.

Starting with $[Ir_2Cl(CO)_4(DPM)_2][X]$, having noncoordination anions (X^- = BF_4^-, BPh_4^-), we might also expect to obtain the cationic tricarbonyl and dicarbonyl complexes analogous to the known rhodium species.[21,22,32] Although CO loss from the tetracarbonyl species occurs to give the tricarbonyl complex **4**, loss of a second CO to give the dicarbonyl A-frame does not occur readily; under refluxing conditions a mixture of products is obtained, one of which is the desired dicarbonyl compound. This again contrasts the behavior of the analogous Rh tricarbonyl species, which loses CO readily to give the dicarbonyl A-frame. However, $[Ir_2(CO)_2(\mu\text{-}Cl)(DPM)_2][BF_4]$ (**5b**) can easily be obtained by chloride abstraction from $[IrCl(CO)(DPM)]_2$ (**3**) using 1 equiv of $AgBF_4$. All evidence suggests an A-frame formulation for **5b** analogous to that of $[Rh_2(CO)_2(\mu\text{-}Cl)(DPM)_2][BF_4]$;[23,32] its infrared spectrum has two terminal carbonyl bands at 1989 and 1964 cm^{-1}, it is a 1:1 electrolyte, and its $^{31}P\{^1H\}$ NMR spectrum indicates that all phosphorus atoms are equivalent. In addition, the stepwise addition of CO to compound **5b** yields the corresponding tricarbonyl complex **4b** and finally the tetracarbonyl species **1b**.

As noted earlier, the $^{31}P\{^1H\}$ chemical shift of **5b** is highly solvent dependent (in CH_2Cl_2, δ 17.26; in acetone, δ 15.80; in THF, δ 12.07). Also, the addition of THF to a CH_2Cl_2 solution of **5b** causes a shift from the CH_2Cl_2-only value to the THF-only value at THF:CH_2Cl_2 volume ratios of 3:2; at no time during these additions were any new peaks observed. Similarly, the addition of acetone caused a shift in the position of the $^{31}P\{^1H\}$ peak at **5b**. With the stronger donor solvent, acetonitrile, the addition of only 100 μL of acetonitrile to a CH_2Cl_2 solution of **5b** (75 mg in 1 mL) caused a shift by approximately δ 15 to δ 2.40. The solution infrared spectrum, however, showed no band attributable to coordinated acetonitrile, and similarly no obvious change in the carbonyl stretches was observed in any of the above additions, suggesting a weak interaction between **5b** and solvent. Solid samples isolated from acetonitrile solutions of **5b** contained no acetonitrile, further indicating only weak interaction between CH_3CN and **5b** in solution. It seems therefore that in coordinating solvents compound **5** interacts with the solvent molecules; however, the number of molecules involved and the site(s) of solvent coordination are not known.

Description of Structure

$[Ir_2Cl_2(CO)_2(\mu\text{-}CO)(DPM)_2]$ crystallized from a THF/ether mixture along with 3 molecules of THF of crystallization. Two of these are planar while the other has a slightly puckered geometry and higher thermal parameters, suggesting a slight disorder of this group. The presence of the two conformations of THF molecules is not unusual, and both have been observed before.[44] Significantly, in the report by Hodgson and Raymond,[44] in which both THF conformations were observed in

---

(41) Cowie, M.; Sutherland, B. R. *Inorg. Chem.* **1984**, *23*, 1290.

(42) Cowie, M.; Sutherland, B. R., unpublished results.

(43) The observed density and the measured cell parameters in fact yield Z = 2.21. This discrepancy probably results from the poorly determined cell parameters derived from film measurements; it may also be that there is solvent of crystallization.

(44) Hodgson, K. O.; Raymond, K. N. *Inorg. Chem.* **1972**, *11*, 171 and references therein.

Table V. Selected Interatomic Distances (Å) in $[Ir_2Cl_2(CO)_3(DPM)_2]\cdot 3C_4H_8O$[a, b]

Ir(1)–Ir(2)	2.779 (1)	P(1)–C(4)	1.82 (2)
Ir(1)–C(3)	2.04 (3)	P(2)–C(4)	1.82 (3)
Ir(2)–C(3)	2.04 (2)	P(3)–C(5)	1.84 (3)
Ir(1)–Cl(1)	2.489 (7)	P(4)–C(5)	1.80 (3)
Ir(1)–Cl(1)′	2.557 (9)	P(1)–C(11)	1.834 (10)
Ir(2)–Cl(2)	2.520 (5)	P(1)–C(21)	1.817 (9)
Ir(2)–Cl(2)′	2.556 (1)	P(2)–C(31)	1.833 (9)
Ir(1)–P(1)	2.341 (3)	P(2)–C(41)	1.819 (10)
Ir(1)–P(3)	2.329 (3)	P(3)–C(51)	1.821 (10)
Ir(2)–P(2)	2.321 (3)	P(3)–C(61)	1.826 (10)
Ir(2)–P(4)	2.331 (3)	P(4)–C(71)	1.813 (13)
C(3)–O(3)	1.20 (4)	P(4)–C(81)	1.823 (13)

[a] All terminal carbonyl groups were input in their idealized positions with distances of Ir–C = 1.82 Å and C–O = 1.15 Å and with Ir–C–O angles of 180°. [b] Interatomic distances (Å) for the THF solvent molecules are listed in the supplementary data.

the same structure, the thermal parameters involving the puckered molecule were significantly higher than those in the planar one, as is observed in our structure. Nevertheless, even the worst THF molecule in our structure has a geometry typically observed for such a group.[30] There are no unusual contacts between the THF molecules and the Ir–DPM complex.

The complex has essentially the geometry expected for a binuclear DPM-bridged compound (see Figures 1 and 2). All Ir–P distances (range 2.321 (3)–2.341 (3) Å) are in agreement with the analogous distances found in another structurally characterized DPM-bridged Ir complex.[17] All P–C distances (see Table V) are normal as are the angles associated with the DPM ligands (Table VI). Both methylene groups of the DPM ligands are bent away from the bridging CO. The orientation of these CH_2 groups is dictated by the positions of the phenyl groups, which are situated such as to minimize contacts with the CO and Cl ligands in the equatorial plane. As noted earlier, the terminal CO positions were idealized while the Cl positions were allowed to vary. All of the resulting Ir–Cl distances (range 2.489 (7)–2.557 (9) Å) are reasonable, and these, together with the refined occupancy factors and thermal parameters of the CO and Cl ligands, suggest that the positioning of the CO groups was fairly accurate. The bridging carbonyl group is quite typical although the slight elongation

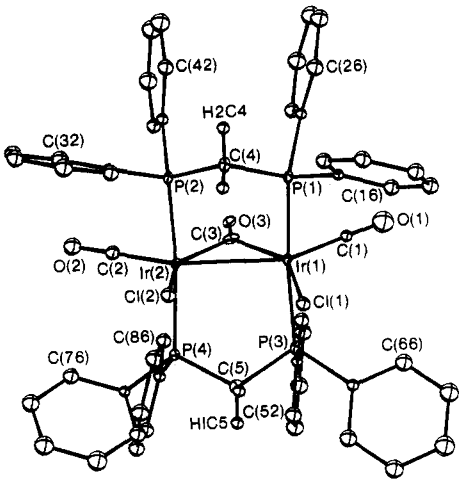

Figure 1. Perspective view of isomer **2a**, $[Ir_2Cl_2(CO)_2(\mu\text{-}CO)(DPM)_2]$ (25% abundance). Thermal ellipsoids are drawn at the 20% level except for methylene hydrogens, which are drawn artificially small on both figures. Phenyl hydrogens have the same number as their attached carbon atoms.

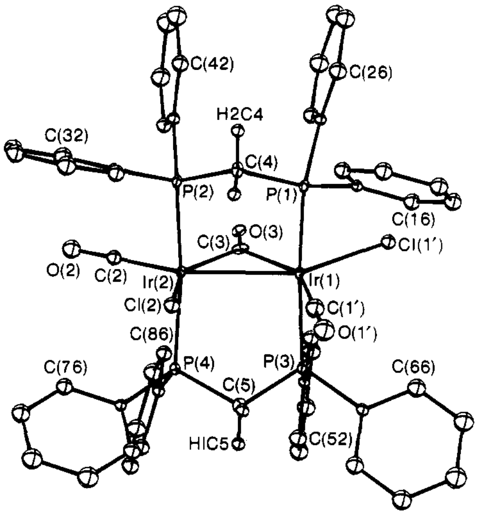

Figure 2. Perspective view of the 75% isomer **2b**, $[Ir_2Cl_2(CO)_2(\mu\text{-}CO)(DPM)_2]$.

Table VI. Selected Angles (deg) in $[Ir_2Cl_2(CO)_3(DPM)_2]\cdot 3C_4H_8O$

Ir(2)–Ir(1)–Cl(1)	97.8 (1)	Ir(1)–Ir(2)–Cl(2)′	146.11 (2)	Ir(1)–C(1)′–O(1)′	*a*	C(11)–P(1)–C(21)	102.4 (4)
Ir(2)–Ir(1)–Cl(1)′	144.6 (2)	Ir(1)–Ir(2)–C(2)	150.08 (2)	Ir(2)–C(2)–O(2)	*a*	C(31)–P(2)–C(41)	101.0 (5)
Ir(2)–Ir(1)–C(1)	143.67 (2)	Ir(1)–Ir(2)–C(2)′	97.91 (2)	Ir(2)–C(2)′–O(2)′	*a*	C(51)–P(3)–C(61)	100.7 (4)
Ir(2)–Ir(1)–Cl(1)′	101.50 (2)	Ir(1)–Ir(2)–C(3)	47.0 (7)	Ir(1)–C(3)–O(3)	138.0 (9)	C(71)–P(3)–C(81)	102.0 (4)
Ir(2)–Ir(1)–C(3)	47.0 (7)	Ir(1)–Ir(2)–P(2)	92.78 (8)	Ir(2)–C(3)–O(3)	136.0 (9)	P(1)–C(4)–P(2)	110.6 (2)
Ir(2)–Ir(1)–P(1)	92.15 (8)	Ir(1)–Ir(2)–P(4)	93.1 (2)	Ir(1)–P(1)–C(4)	112.2 (6)	P(3)–C(4)–P(4)	110.9 (3)
Ir(2)–Ir(1)–P(3)	92.08 (9)	Cl(2)–Ir(2)–C(2)	114.86 (8)	Ir(2)–P(2)–C(4)	109.9 (7)	P(1)–C(11)–C(12)	121.6 (3)
Cl(1)–Ir(1)–C(1)	118.5 (1)	Cl(2)′–Ir(2)–C(2)′	115.98 (2)	Ir(1)–P(3)–C(5)	109.1 (8)	P(1)–C(11)–C(16)	118.5 (4)
Cl(1)–Ir(1)–C(1)′	113.8 (2)	Cl(2)–Ir(2)–C(3)	141.9 (7)	Ir(2)–P(4)–C(5)	111.0 (7)	P(1)–C(21)–C(22)	119.9 (3)
Cl(1)–Ir(1)–C(3)	144.5 (7)	Cl(2)′–Ir(2)–C(3)	99.1 (7)	Ir(1)–P(1)–C(11)	113.1 (2)	P(1)–C(21)–C(26)	119.8 (5)
Cl(1)′–Ir(1)–C(3)	97.9 (7)	C(2)–Ir(2)–C(3)	103.0 (7)	Ir(1)–P(1)–C(21)	120.1 (3)	P(2)–C(31)–C(32)	117.0 (5)
C(1)–Ir(1)–C(3)	96.8 (7)	C(2)′–Ir(2)–C(3)	144.8 (7)	Ir(2)–P(2)–C(31)	114.1 (3)	P(2)–C(31)–C(36)	122.9 (4)
C(1)′–Ir(1)–C(3)	148.1 (6)	P(2)–Ir(2)–P(4)	168.4 (3)	Ir(2)–P(2)–C(41)	119.7 (3)	P(2)–C(41)–C(42)	120.2 (5)
P(1)–Ir(1)–P(3)	168.8 (2)	P(2)–Ir(2)–Cl(2)	83.7 (1)	Ir(1)–P(3)–C(51)	120.8 (3)	P(2)–C(41)–C(46)	119.8 (3)
P(1)–Ir(1)–Cl(1)	86.9 (2)	P(2)–Ir(2)–Cl(2)′	91.1 (1)	Ir(1)–P(3)–C(61)	115.9 (3)	P(3)–C(51)–C(52)	121.3 (3)
P(1)–Ir(1)–Cl(1)′	88.3 (2)	P(4)–Ir(2)–Cl(2)	85.8 (3)	Ir(2)–P(4)–C(71)	111.8 (2)	P(3)–C(51)–C(56)	118.7 (5)
P(3)–Ir(1)–Cl(1)	82.2 (2)	P(4)–Ir(2)–Cl(2)′	89.6 (2)	Ir(2)–P(4)–C(81)	120.8 (3)	P(3)–C(61)–C(62)	121.6 (4)
P(3)–Ir(1)–Cl(1)′	94.3 (2)	P(2)–Ir(2)–C(2)	89.3 (1)	C(4)–P(1)–C(11)	102.9 (9)	P(3)–C(61)–C(66)	118.0 (4)
P(1)–Ir(1)–C(1)	89.27 (9)	P(2)–Ir(2)–C(2)′	83.0 (1)	C(4)–P(1)–C(21)	104.2 (8)	P(4)–C(71)–C(72)	123.0 (4)
P(1)–Ir(1)–C(1)′	87.1 (1)	P(4)–Ir(2)–C(2)	90.6 (2)	C(4)–P(2)–C(31)	104.8 (9)	P(4)–C(71)–C(76)	117.0 (5)
P(3)–Ir(1)–C(1)	93.5 (1)	P(4)–Ir(2)–C(2)′	86.3 (3)	C(4)–P(2)–C(41)	106.0 (8)	P(4)–C(81)–C(82)	118.4 (5)
P(3)–Ir(1)–C(1)′	81.9 (1)	P(2)–Ir(2)–C(3)	93.8 (5)	C(5)–P(3)–C(51)	104.9 (11)	P(4)–C(81)–C(86)	121.6 (4)
P(1)–Ir(1)–C(3)	97.8 (5)	P(4)–Ir(2)–C(3)	97.5 (6)	C(5)–P(3)–C(61)	103.6 (10)		
P(3)–Ir(1)–C(3)	92.7 (5)	Ir(1)–C(3)–Ir(2)	85.95 (3)	C(5)–P(4)–C(71)	104.5 (10)		
Ir(1)–Ir(2)–Cl(2)	95.03 (8)	Ir(1)–C(1)–O(1)	*a*	C(5)–P(4)–C(81)	105.3 (10)		

[a] Idealized 180°.

of the C(3) thermal ellipsoid parallel to the Ir–Ir vector probably disguises a slight disorder of this group. It is to be expected that the CO parameters trans to another CO should differ slightly compared to those when it is trans to a Cl ligand. It is not unexpected then that the disorder of the terminal CO and Cl groups should result in a slight disorder of the bridging CO group. Nevertheless, only one atom position was observed for each of C(3) and O(3), and the parameters associated with this group are normal. The Ir–C(3) distances (2.04 (3) Å) and the C(3)–O(3) distance (1.20 (4) Å) are normal for such groups and are, as expected, longer than those involving terminal CO groups. The acute Ir(1)–C(3)–Ir(2) angle of 85.95 (3)° is typical of bridging CO's when accompanied by a metal–metal bond.

The Ir(1)–Ir(2) distance (2.779 (1) Å) is normal for a single bond and is significantly less than that observed in the similar compound $[Ir_2(CO)_2(\mu\text{-}S)(\mu\text{-}CO)(DPM)_2]$[17] in which the large bridging sulfide group forces the metals apart somewhat. The metal–metal distance in the present compound is substantially less than the intraligand P–P distances (average 2.996 (5) Å), indicating compression along the Ir–Ir axis due to the metal–metal interaction.

As indicated, the present structure is disordered in the solid state such that there are two chemically distinct species in approximately a 75:25 ratio, with the minor isomer having all carbonyls mutually cis while in the major isomer one of the terminal carbonyls is trans to the bridging CO and the other is cis to it (see Figures 1 and 2 for views of the two isomers). In the solid state the major isomer is further disordered such that there are the three contributing structures in the solid state (I–III). These structures clearly explain the 50% occupancies of C(1)–O(1), C(1)′–O(1)′, Cl(1), and Cl(1)′ and the 75:25 occupancies of C(2)–O(2), Cl(2), and their primed counterparts. Chemically, the second and third structures (II and III) are identical so that only two sets of carbonyl bands are observed, one for each isomer. In the infrared spectrum of the solid these are observed in approximately the correct intensity ratios with the CO bands due to the trans isomer more intense than those of the cis isomer, while in CH_2Cl_2 solution their intensities are approximately the same, indicating an equal abundance (vide supra).

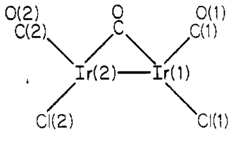

I (25%)

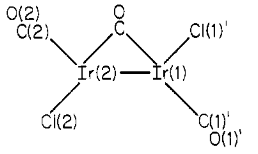

II (50%)

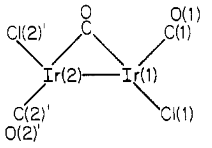

III (25%)

Although the terminal carbonyl and chloro ligands are disordered in this structure, this X-ray determination is nevertheless a significant one. It clearly establishes the geometry of the complex and demonstrates in these DPM-bridged complexes the higher coordination that is favored for Ir over that for Rh. The analogous compound for Rh has only one of the chloride ligands coordinated in the bridging position with the other as a Cl^- counterion. This structure also represents the first reported for which the $Ir_2(DPM)_2$ framework has a bridging equatorial ligand and *two* terminal ligands on each metal and therefore supports the formulation proposed for the tetracarbonyl complex **1** and also those proposed for a series of analogous isocyanide adducts.[6] In addition, the disorder that plagued the structural determination did prove beneficial in explaining the spectral parameters observed for compounds **2a** and **2b**.

Conclusions

We have now clearly established the identities of a series of neutral and cationic binuclear chloro carbonyl complexes of iridium and have developed reasonable synthetic routes to these complexes. Although there are many close analogies to the Rh–DPM chemistry, there are also significant differences related to the higher basicity of the Ir atoms compared to Rh, causing the Ir complexes to bind CO more strongly. This latter tendency suggests and even richer chemistry of these complexes with small molecules than was observed for the Rh system. Many of the above reported complexes have already been observed to react smoothly with acetylenes,[38] olefins,[39] H_2,[37] and heteroallenes.[39] Full details of these reactions will be the subject of future reports.

Acknowledgment. This work was supported by The University of Alberta and the Natural Sciences and Engineering Research Council of Canada. We thank the NSERC for a graduate scholarship to B.R.S. and Dr. R. G. Ball for collecting the X-ray data.

Supplementary Material Available: Listings of observed and calculated structure factors, U_{ij}'s and associated standard deviations of the anisotropic atoms, interatomic distances for the THF rings, and idealized hydrogen parameters (19 pages). Ordering information is given on any current masthead page.